Myeloperoxidase-catalyzed oxidation of cyanide to cyanate: A potential carbamylation route involved in the formation of atherosclerotic plaques?

Received for publication, June 8, 2017, and in revised form, February 20, 2018 Published, Papers in Press, March 1, 2018, DOI 10.1074/jbc.M117.801076

Cédric Delporte[a,b1,2], Karim Zouaoui Boudjeltia[c1], Paul G. Furtmüller[d], Richard A. Maki[e,f], Marc Dieu[g], Caroline Noyon[a3], Monika Soudi[d], Damien Dufour[a,b], Catherine Coremans[a,b3], Vincent Nuyens[c], Florence Reye[a], Alexandre Rousseau[c], Martine Raes[g], Nicole Moguilevsky[h], Michel Vanhaeverbeek[c], Jean Ducobu[c], Jean Nève[a], Bernard Robaye[i], Luc Vanhamme[i4], Wanda F. Reynolds[f], Christian Obinger[d1], and Pierre Van Antwerpen[a,b1,5]

From the [a]Laboratory of Pharmaceutical Chemistry and [b]Analytical Platform, Faculty of Pharmacy, Université Libre de Bruxelles, 1050 Brussels, Belgium, the [c]Laboratory of Experimental Medicine, CHU de Charleroi, A. Vésale Hospital, Université Libre de Bruxelles, 6110 Montigny-le-Tilleul, Belgium, the [d]Department of Chemistry, Division of Biochemistry, University of Natural Resources and Life Sciences (BOKU), 1180 Vienna, Austria, [e]Torrey Pines Pharmaceuticals, Del Mar, California 92014, the [f]Sanford-Burnham-Prebys Medical Discovery Institute, La Jolla, California 92037, the [g]Laboratory of Cellular Biology and [h]Technology Transfer Office, University of Namur, 5000 Namur, Belgium, the [i]Institute of Interdisciplinary Research, Institut de Recherche Interdisciplinaire en Biologie Humaine et Moléculaire, Faculty of Sciences, Université Libre de Bruxelles, 6041 Gosselies, Belgium, and the [j]Laboratory of Molecular Parasitology, Institut de Recherche Interdisciplinaire en Biologie Humaine et Moléculaire, Faculty of Sciences, Université Libre de Bruxelles, 6041 Gosselies, Belgium

Edited by Ruma Banerjee

Protein carbamylation by cyanate is a post-translational modification associated with several (patho)physiological conditions, including cardiovascular disorders. However, the biochemical pathways leading to protein carbamylation are incompletely characterized. This work demonstrates that the heme protein myeloperoxidase (MPO), which is secreted at high concentrations at inflammatory sites from stimulated neutrophils and monocytes, is able to catalyze the two-electron oxidation of cyanide to cyanate and promote the carbamylation of taurine, lysine, and low-density lipoproteins. We probed the role of cyanide as both electron donor and low-spin ligand by pre-steady-state and steady-state kinetic analyses and analyzed reaction products by MS. Moreover, we present two further pathways of carbamylation that involve reaction products of MPO, namely oxidation of cyanide by hypochlorous acid and reaction of thiocyanate with chloramines. Finally, using an *in vivo* approach with mice on a high-fat diet and carrying the human MPO gene, we found that during chronic exposure to cyanide, mimicking exposure to pollution and smoking, MPO promotes protein-bound accumulation of carbamyllysine (homocitrulline) in atheroma plaque, demonstrating a link between cyanide exposure and atheroma. In summary, our findings indicate that cyanide is a substrate for MPO and suggest an additional pathway for *in vivo* cyanate formation and protein carbamylation that involves MPO either directly or via its reaction products hypochlorous acid or chloramines. They also suggest that chronic cyanide exposure could promote the accumulation of carbamylated proteins in atherosclerotic plaques.

Carbamylation is a post-translational modification of biological molecules bearing an amino group. It occurs in several physio- and/or pathophysiological conditions. For example, it is well known that the ϵ-amino group of lysine residues of proteins can be converted to carbamyllysine (1–4), also named homocitrulline (Hcit),[6] and that chronic renal insufficiency correlates with enhanced carbamylation mediated by urea-derived cyanate ($^{-}$O–C≡N). In patients with renal disease, carbamylation of low-density lipoproteins (LDLs) is considered as a nontraditional risk factor for cardiovascular insufficiency. It manifests all of the biological effects relevant to atherosclerosis, including endothelial cell injuries, expression of adhesion molecules, and vascular smooth muscle cell proliferation (5). Carbamylation of type I collagen has been shown to induce conformational changes and reduce its ability to activate human

This study was supported by Austrian Science Funds Grant FWF P 20664 (to P. G. F.) and doctoral program BioToP Grant W1224 (to M. S.), Belgian National Fund for Scientific Research (FRS) Grants 3.4553.08 and T.0136.13 PDR, Université Libre de Bruxelles Grant FER-207, and Department of International Relationships of the Université Libre de Bruxelles Grant BRIC SJ/AL/BRIC/130. This study was also supported in part by National Institutes of Health Grants RO1-NS074303 (to W. F. R.) and R43 AG040935 (to R. A. M.). This work was also supported by the Institute of Pathology and Genetics (IRSPG, Loverval, Belgium) and the "CHU of Charleroi." Additional funds to support this work were provided by Sanford Burnham Prebys Medical Discovery Institute. The authors declare that they have no conflicts of interest with the contents of this article. The content is solely the responsibility of the authors and does not necessarily represent the official views of the National Institutes of Health.

This article contains Figs. S1–S5.

[1] These authors contributed equally to this work.

[2] Postdoctoral researcher supported by the Belgian Fund for Scientific Research (FRS-FNRS).

[3] Research Fellow of FRS-FNRS.

[4] Research Director of FRS-FNRS.

[5] To whom correspondence should be addressed: Laboratory of Pharmaceutical Chemistry and Analytical Platform, Faculty of Pharmacy, Université Libre de Bruxelles, Brussels, Belgium. Tel.: 3226505263; Fax: 32265052489; E-mail: pvantwer@ulb.ac.be.

[6] The abbreviations used are: Hcit, homocitrulline; LDL, low-density lipoprotein; MPO, myeloperoxidase; LS, low-spin; EPO, eosinophil peroxidase; LPO, lactoperoxidase; ESI, electrospray ionization; QTOF, quadrupole TOF; LDLR, LDL receptor; HRP, horseradish peroxidase; CE, collision energy.

polymorphonuclear neutrophils involved in the immune response (6).

Recently, myeloperoxidase (MPO) has been demonstrated to be indirectly involved in protein carbamylation (7). This enzyme, a member of the peroxidase-cyclooxygenase superfamily (8), is secreted at inflammatory sites from stimulated neutrophils and also from monocytes (9). It catalyzes the two-electron oxidation of thiocyanate ($^{-}$S–C≡N), thereby producing hypothiocyanous acid (HO–S–C≡N) and cyanate as a minor by-product (7). Protein carbamylation may therefore be driven not only by uremia but also by inflammation. Upon exposure of LDL to either MPO/H_2O_2/$^{-}$SCN or the potassium salt of $^{-}$O–C≡N, protein recognition by LDL receptor was attenuated, whereas its interaction with the scavenger receptor SR-A1 was enhanced. A clear relationship between the plasma levels of protein-bound ϵ-carbamyllysine (Hcit) and an increased risk of cardiovascular disease could be established (7).

We hereafter demonstrate the existence of a new alternative mechanism for cyanate formation and potential protein carbamylation at sites of inflammation, according to the following reaction, which involves the hydrogen peroxide–mediated oxidation of cyanide ($^{-}$C≡N) catalyzed by MPO (Reaction 1).

$$H\text{–}O\text{–}O\text{–}H + {}^{-}C{\equiv}N \xrightarrow{MPO} {}^{-}O\text{–}C{\equiv}N + H\text{–}O\text{–}H$$

Reaction 1

Cyanide is well known as a product of organic material combustion (10) (atmospheric pollution, tobacco smoking) or from intake of cyanogenic glycosides (almond) (11). *In vivo*, it is a universal ligand able to bind to and inhibit heme enzymes. Exposure to high concentrations results in death within seconds to minutes by impairment of dioxygen (O_2) distribution within the body and inhibition of the respiratory electron transport chain in the mitochondria (12). Five-coordinated ferric high-spin heme proteins (*e.g.* cytochrome *c* oxidase, methemoglobin, metmyoglobin, catalase, peroxidases, etc.) are its preferential targets. Cyanide, which at most biological pH levels is protonated (pK_a = 9.14), binds as an anion to Fe(III) and transforms the corresponding heme protein into its six-coordinated low-spin (LS) form, thereby impeding the interaction with natural substrates (*e.g.* O_2 or H_2O_2). The binding rates and complex equilibria involved are very variable. Typically, eukaryotic peroxidases (including MPO) and catalases bind cyanide rapidly (1.1×10^5 M^{-1} s^{-1} to 1.3×10^6 M^{-1} s^{-1}) (13–17), taking up both the anion and a proton (18). So far, this LS complex formation has been thought to effectively block the redox chemistry of all heme enzymes without any exceptions (K_D = 1–10 μM). However, the present study unequivocally demonstrates that cyanide can act both as ligand of MPO and electron donor to compound I of MPO.

Myeloperoxidase is a unique oxidoreductase in human physiology. The reconstructed phylogeny of mammalian peroxidases indeed demonstrates that MPOs form a well-separated clade within the vertebrate peroxidases (*i.e.* Family 1 of the peroxidase-cyclooxygenase superfamily) (8). This superfamily also includes peroxidasins, peroxinectins, cyclooxygenases, and dual oxidases (8). Fig. 1*A* depicts the family of vertebrate peroxidases, with the clades of myeloperoxidases and eosinophil peroxidases (EPOs) being well separated from the other branches. Segregation of MPO is well reflected by its unique biophysical and biochemical properties (19) that are closely related to its physiological role and the nature of its substrates. It participates in innate immune defense mechanisms through formation of microbicidal-reactive oxidants and diffusible radical species. Its unique substrate is chloride that is oxidized to antimicrobial hypochlorous acid (HOCl). Chloride oxidation is a thermodynamically challenging reaction that requires the formation of strong oxidizing redox intermediates (*i.e.* the so-called "compound I" formed by oxidation of ferric MPO by hydrogen peroxide) (Fig. 2*A*) (20). The standard reduction potential of the couple compound I/MPO(III) ($E^{\circ\prime}$ = 1.16 V) provides the driving force of this reaction (Fig. 2*A*). Moreover, as will be demonstrated below, it also uniquely enables MPO to oxidize cyanide to cyanate, thereby contributing to a so far unknown route for protein carbamylation. The presented data also suggest multiple pathways of cyanate formation and protein carbamylation that involve MPO either directly or its reaction products hypochlorous acid and/or chloramine. Experiments in mouse model demonstrate the relevance of these pathways *in vivo* as cyanide is directly metabolized and promotes accumulation of protein-bound Hcit in atheroma plaque.

Results

Hydrogen peroxide consumption mediated by cyanide

In a preliminary study, the consumption of hydrogen peroxide by MPO, promoted by cyanide, was probed by amperometric monitoring. Fig. 1*B* clearly shows that 0.5 μM MPO consumes 100 μM H_2O_2 within 300 s in the presence of 100 μM cyanide, whereas no effect is observed under identical conditions with related enzymes, such as lactoperoxidase (LPO) and EPO. At lower cyanide concentrations (50–100 μM), MPO rapidly consumes H_2O_2, whereas the inhibitory effect is evident at higher concentrations (500–1000 μM; Fig. 1*B*). The slow H_2O_2 consumption observed in control experiments (absence of cyanide) is due to the well-known low (pseudo)catalase activity of mammalian peroxidases (20).

Cyanide acts as electron donor for MPO compound I

Myeloperoxidase catalyzes one- and two-electron oxidation reactions (Fig. 2*A*). The relevant redox intermediate involved in both reactions (compound I; *i.e.* an oxoiron(IV) porphyrin radical cation) is formed via a two-electron oxidation of the ferric enzyme (PorFe(III)) by H_2O_2.

$$PorFe(III) + H_2O_2 \xrightarrow{k_1} {}^{+\cdot}PorFe(IV){=}O + H_2O$$

Reaction 2

In two-electron transitions, compound I (about 50% hypochromicity of Soret band compared with ferric MPO) is directly reduced to ferric MPO (Soret band at 428 nm), whereas in one-electron transitions, compound II (Soret band at 456 nm) is

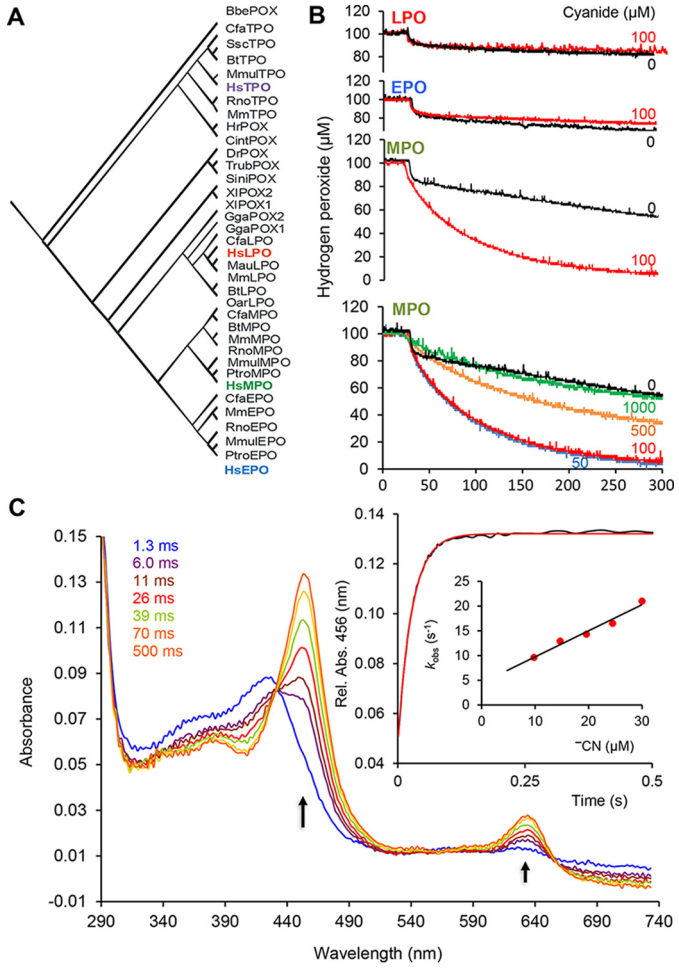

Figure 1. *A*, reconstructed phylogenetic tree showing the family of vertebrate peroxidases, including the mammalian enzymes MPO, EPO, LPO, and thyroid peroxidase (*TPO*). *B*, amperometric measurements (650 mV) of the H_2O_2 consumption in the presence of 0.5 μM peroxidases (LPO, EPO, or MPO), 100 μM H_2O_2, and $^{-}$CN at various concentrations. *C*, reaction of 2 μM MPO compound I with 50 μM cyanide followed in the sequential-mixing stopped-flow mode. Conditions were as follows: 100 mM phosphate buffer, pH 7.0, 25 °C. *Arrows*, wavelength with absorbance changes. The first spectrum was taken 1.3 ms after mixing. *Inset*, typical time trace followed at 456 nm (maximum absorbance of MPO(III)-cyanide complex) and plot of the pseudo-first-order rate constants, k_{obs}, *versus* cyanide concentrations.

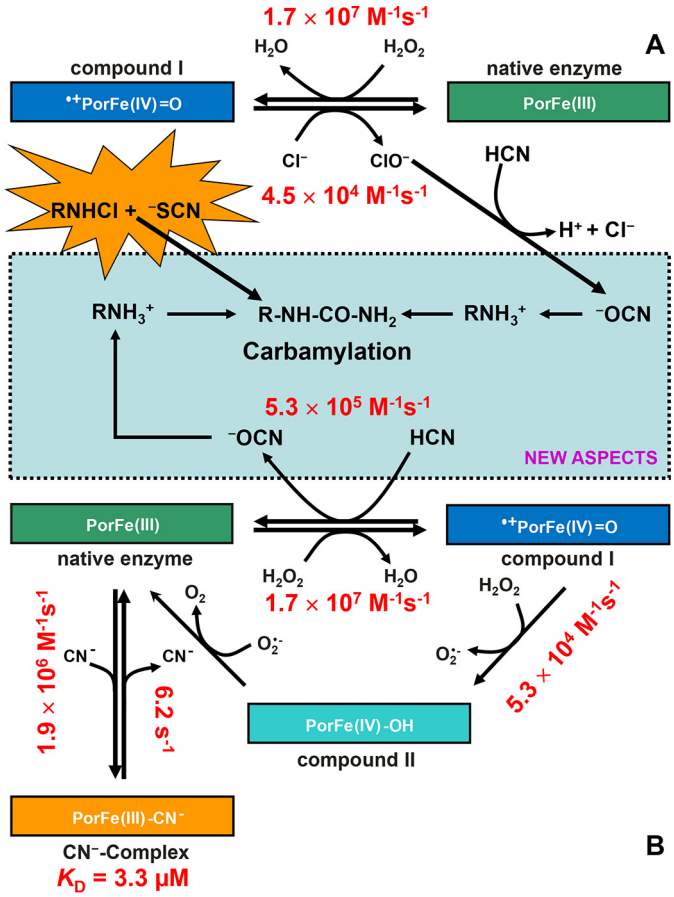

Figure 2. Carbamylation promoted by the system MPO/H_2O_2/$^{-}$CN system and MPO-typical reaction products. *A*, MPO-typical oxidation of chloride to hypochlorous acid (*i.e.* chlorination cycle). Ferric MPO (PorFe(III)) is oxidized to compound I ($^{+}$PorFe(IV)=O; oxoiron(IV) porphyrin radical), which is directly reduced to the resting state by chloride, thereby releasing hypochlorous acid (HOCl/$^{-}$OCl). Hypochlorous acid mediates the oxidation of cyanide to cyanate and the formation of chloramines, which may be also involved in carbamylation by direct reaction with thiocyanate (*NEW ASPECTS*). *B*, two-electron oxidation of cyanide to cyanate by MPO compound I, thereby restoring the ferric protein and releasing cyanate (5.3 × 10^5 M^{-1} s^{-1}; *NEW ASPECTS*). Ferric MPO binds cyanide, forming the low-spin complex (PorFe(III)-CN^{-}, K_D = 3.3 μM). Further MPO-typical reactions include the one-electron reduction of compound I to compound II by H_2O_2 (14) or by other one-electron donors followed by compound II reduction to ferric MPO. Kinetic constants were calculated from current experiments (see "Experimental procedures") or from the literature when already known (13–17).

formed. These reactions can easily be probed by sequential stopped-flow spectroscopy. Fig. 1*C* shows a representative series of spectra obtained by mixing 4 μM MPO compound I with 100 μM cyanide. The reaction is monophasic and linearly dependent on cyanide concentration. It rapidly forms a MPO species that had its Soret band at 456 nm, which could derive from either compound II or the LS complex between ferric MPO and cyanide (19). The determined apparent bimolecular rate constant is (5.3 ± 0.5) × 10^5 M^{-1} s^{-1} at pH 7.0 and 25 °C. It is unlikely that cyanide mediates the reduction of compound I to compound II, because this reaction is thermodynamically unfavorable (see below). Moreover, the reaction of preformed compound II with cyanide probed in the sequential stopped-flow mode clearly demonstrated that compound II does not participate in the turnover of the MPO/H_2O_2/$^{-}$CN system. By contrast, the observed spectral transition suggests the cyanide-mediated direct reduction of compound I to ferric MPO. The latter rapidly binds excess cyanide, forming the LS complex with Soret maximum at 456 nm (see also Figs. S4 and S5).

For comparison, the reaction of cyanide with preformed compound I of LPO and EPO as well as horseradish peroxidase (a model plant-type peroxidase) was also investigated under identical conditions. With LPO and EPO, compound I is slowly transformed to compound II (2 s^{-1}), which is a well-known phenomenon of intramolecular electron transport in the absence of exogenous electron donors (21–23) (see Fig. 1*A*). Horseradish peroxidase compound I is stable in the presence of cyanide (see Fig. S1*B*).

MPO-mediated cyanide oxidation generates cyanate

To prove direct reduction of compound I to ferric MPO and concomitant two-electron oxidation of cyanide to $^{-}$OCN, MPO was incubated with both H_2O_2 and the isotopomers

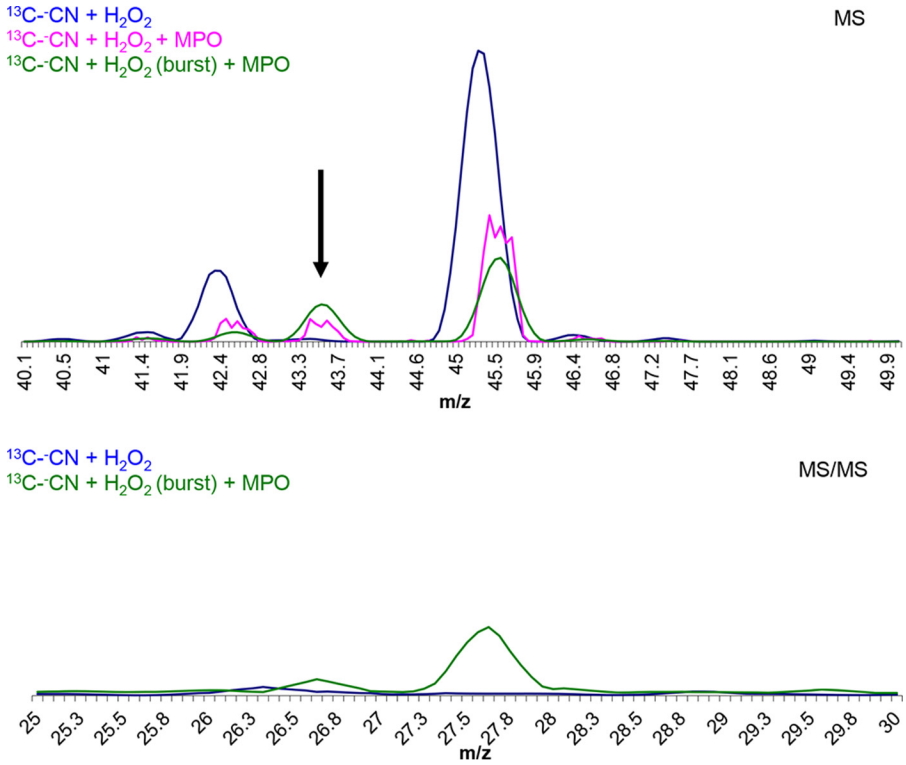

Figure 3. Tandem MS/MS determination of cyanate production. MS spectra show a peak around 43 *m/z* corresponding to ^{13}C-cyanate, when MPO (1 μM) was added to a mixture of [^{13}C]cyanide (2 mM) and H_2O_2 (200 μM) (*pink solid line*). Results obtained upon the repeated addition of H_2O_2 (three times) are depicted by the *green solid line*. MS/MS spectra show a peak around 27 *m/z* corresponding to the fragmentation of [^{13}C]cyanate into [^{13}C]cyanide (*green solid line*).

$^{-}$CN, [^{13}C]$^{-}$CN, or [^{13}C,^{15}N]$^{-}$CN. The reaction products were analyzed by MS. Fig. 3 shows the formation of a reaction product with an appropriate *m/z* (*i.e.* *m/z* = 43) and a fragment ion at *m/z* = 27. Fig. 4*A* illustrates the formation of cyanate using the three isotopomers. Upon using $^{-}$CN, [^{13}C]$^{-}$CN, or [^{13}C,^{15}N]$^{-}$CN, peaks at *m/z* values of 41.999, 43.002, or 43.999 were found, clearly demonstrating the formation of the isotopomers $^{-}$OCN, [^{13}C]$^{-}$OCN or [^{13}C,^{15}N]$^{-}$OCN, respectively. In the absence of cyanide or hydrogen peroxide or MPO, no cyanate was produced except for hydrogen peroxide with cyanide, where a low cyanate production was detected (around 1%). Furthermore, using a calibration curve of cyanate, we were able to calculate that around 13% of cyanide is transformed to cyanate (n = 3) after 1 h (see supporting data for detailed results). These findings clearly indicate that the system MPO/H_2O_2/cyanide is able to produce cyanate and that the conversion of cyanide to cyanate is incomplete (Fig. 4*A*).

Carbamylation of taurine, lysine, and LDL

Furthermore, cyanate produced by MPO-mediated cyanide oxidation was probed in its reaction with nucleophilic amino groups in both taurine and lysine. Taurine is a low-molecular weight amine abundant in millimolar concentration in the cytosol of neutrophils (24). In this study, taurine was used as a chemical model of monoamine because it is stable and its chlorination is well documented. Taurine (1 mM) was incubated with MPO (0.3 μM), hydrogen peroxide (1 mM) and [^{12}C]$^{-}$CN, [^{13}C]$^{-}$CN, or [^{13}C,^{15}N]$^{-}$CN (1 mM) in ammonium acetate buffer, pH 7.4, and the reaction mixture was analyzed by electrospray ionization (ESI)-quadrupole TOF (QTOF) MS in negative mode. Peaks at expected *m/z* values of 167.0109, 168.0284, and 169.0155 corresponding to ^{12}C-, ^{13}C-, and ^{13}C,^{15}N-carbamylated taurine were found (Fig. 4*B*). To further confirm the formation of carbamylated taurine, the isolated peaks were fragmented, leading to peaks with *m/z* values of 124.0074 and 79.9581, respectively, that fully matched with fragments obtained from standard carbamylated taurine (Fig. 4*C*). Similar experiments performed with lysine demonstrated the formation of Hcit (Fig. S2). In the absence of either hydrogen peroxide or MPO, carbamylation of taurine or lysine was negligible or diminished.

Another tested target for carbamylation was LDL. LDLs were incubated with the MPO/H_2O_2/cyanide system before being delipidated and hydrolyzed. Subsequently, the formation of protein-bound Hcit was analyzed by MS and correlated with the abundance of protein-bound lysine by monitoring the ratio Hcit/Lys. A low amount of Hcit was detected in native LDLs. The incubation of LDLs with MPO, H_2O_2, and increasing concentrations of cyanide led to increasing Hcit/Lys ratios (1.5- and 12-fold increases; Fig. 5*A*). The addition of chloride (150 mM) to the MPO/H_2O_2 system in the presence of 100 μM cyanide even increased the extent of carbamylation. Similar levels of carbamylation were observed when LDLs were incubated with HOCl and cyanide (100 μM) (Fig. 5*A*). In the absence of MPO, the Hcit concentration was almost identical to that of native LDLs (data not shown). Furthermore, a positive control with 100 μM of cyanate ($^{-}$OCN) was analyzed. This concentra-

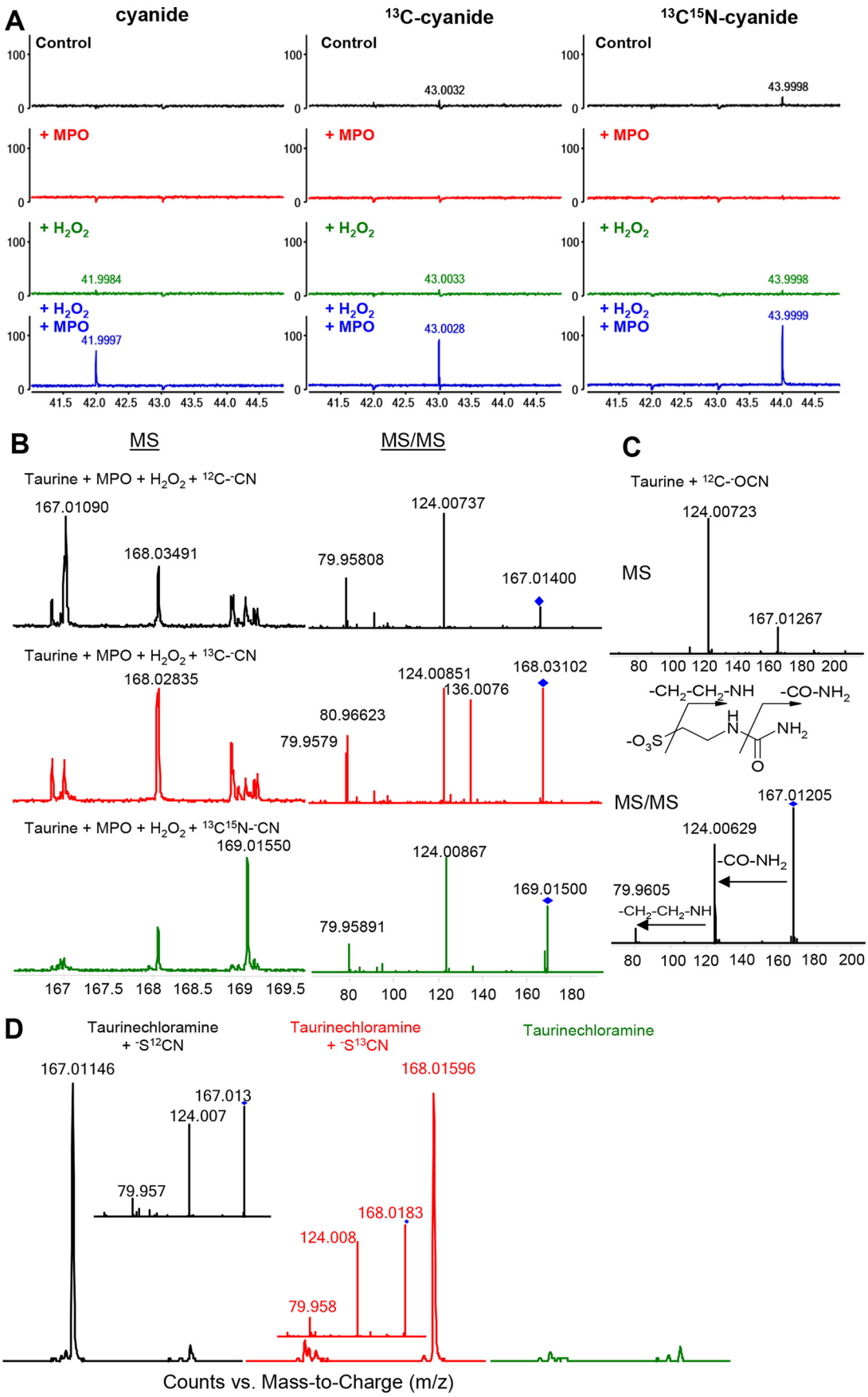
A
cyanide
13C-cyanide
13C15N-cyanide
Control
+ MPO
+ H2O2
+ H2O2 + MPO
41.9984
41.9997
43.0032
43.0033
43.0028
43.9998
43.9999
B
MS
MS/MS
Taurine + MPO + H2O2 + 12C-CN
167.01090
168.03491
124.00737
79.95808
167.01400
Taurine + MPO + H2O2 + 13C-CN
168.02835
124.00851
136.0076
168.03102
80.96623
79.9579
Taurine + MPO + H2O2 + 13C15N-CN
169.01550
124.00867
169.01500
79.95891
C
Taurine + 12C-OCN
124.00723
MS
167.01267
-CH2-CH2-NH
-CO-NH2
-O3S
NH2
MS/MS
167.01205
124.00629
-CO-NH2
79.9605
-CH2-CH2-NH
D
Taurinechloramine + -S12CN
Taurinechloramine + -S13CN
Taurinechloramine
167.01146
167.013
124.007
79.957
168.01596
168.0183
124.008
79.958
Counts vs. Mass-to-Charge (m/z)

tion was used supposing the full conversion of cyanide to cyanate. Surprisingly, this experiment showed a lower carbamylation compared with the MPO/H_2O_2/cyanide/chloride system but a 3 times higher carbamylation when compared with the MPO/H_2O_2/cyanide system (Fig. 5*A*).

The quantitative approach of Hcit formation enabled us to observe that approximately 0.7% of thiocyanate (100 μM) mediated the formation of Hcit in the presence of MPO and H_2O_2. When cyanide was added in the same concentration as thiocyanate (100 μM), the thiocyanate-mediated formation of Hcit decreased to 0.35%; however, the cyanide-mediated formation of Hcit increased to 0.7%. If the thiocyanate concentration was increased to 400 μM, the thiocyanate-mediated formation of Hcit increased to 0.4%, whereas the cyanide-mediated formation decreased to 0.4%. These results highlight the importance of generated HOCl for the Hcit formation mediated by cyanide. Finally, the positive control using cyanate to carbamylate LDLs at 100 μM revealed that only 0.1% of cyanate was converted into Hcit under the conditions used.

Finally, we tested the contribution of each anion (thiocyanate, cyanide, and chloride) in the carbamylation process. Upon the addition of cyanide to the system MPO/H_2O_2/thiocyanate, the contribution of thiocyanate in the carbamylation process decreased (Fig. 5*B*, *left*). However, this was compensated by cyanide-mediated carbamylation, as illustrated by an increase of labeled and total Hcit content (labeled and not labeled; Fig. 5, *B* (*right*) and *C*). Interestingly, when chloride (150 mM) was added in addition to cyanide to the MPO/H_2O_2/thiocyanate system, there was a drop in the formation of Hcit from thiocyanate (Fig. 5*B*, *left*). However, the total carbamylation content increased (total Hcit; Fig. 5*B*, *right*) as cyanide-dependent formation of Hcit (Fig. 5*C*) increased.

Role of hypochlorous acid and chloramines in carbamylation pathways

Hypochlorous acid (HOCl) is an important reaction product of MPO deriving from the two-electron oxidation of chloride by compound I. It is well known that HOCl reacts with amines forming chloramines (*e.g.* taurine chloramines) that in addition contribute to the antimicrobial activity of MPO (25). We could demonstrate that HOCl but not monochloramine is another oxidant of cyanide. Upon mixing hypochlorous acid and cyanide with taurine, carbamylation of taurine is observed (Fig. S3). Actually, HOCl promotes the formation of cyanate from cyanide (Fig. S3). As demonstrated above, formation of Hcit is observed upon incubation of LDL with HOCl and cyanide (Fig. 5*A*).

Additionally, carbamylation can derive from the reaction between thiocyanate and monochloramine. Fig. 4*D* shows the formation of carbamylated adducts with *m*/*z* values of 167.0115 and 168.0160 by using ^{12}C- or ^{13}C-labeled thiocyanate and taurine mono-chloramine. Incubating HOCl-oxidized LDL with thiocyanate increases the Hcit/lysine ratio (Fig. 5*B*).

Cyanide exposure promotes protein-bound carbamylation in atheroma plaque

To confirm that those reactions participate in formation of carbamylated proteins *in vivo*, we used humanized MPO mice transgenic for the intact human MPO gene (−463G allele) (hMPO-TG) with native promoter elements. The rationale for using the hMPO-TG mice is that the human MPO gene is expressed in macrophages in atherosclerotic plaques, whereas the mouse MPO gene is not expressed. This is thought to be due in part to a primate-specific Alu element with binding sites for SP1 and nuclear receptors, including PPARγ (26). Prior studies show MPO presence in atherosclerotic plaques in the MPOG-LDLR$^{-/-}$ model correlating with increased atherosclerotic plaque and hyperlipidemia (27). This cross was used in an earlier study that found increased protein-bound homocitrulline content in atheroplaque laden aorta in huMPOG-LDLR$^{-/-}$ mice as compared with LDL receptor– deficient LDLR$^{-/-}$ controls (7). In this experiment, control mice, human MPO transgenics (−463G allele) (hMPO-TG) mice, and hMPO-TG crossed to the LDLR$^{-/-}$ mice (all on C57BL/6 background) were treated with [^{13}C,^{15}N]cyanide (0.4 mg/kg everyday, ~5 μg/day) or PBS as negative control for 8 weeks (see "Experimental procedures"). Furthermore, mice were exposed to acute inflammation before sacrifice using intraperitoneal injection of zymosan as in prior studies (Wang *et al.* (7) with slight modifications). Protein-bound [^{13}C,^{15}N]Hcit was analyzed in plasma, in atheroma plaques, and in the supernatant and cell pellets of peritoneal lavages. Fig. 6*A* shows that hMPO-TG-LDLR$^{-/-}$ mice treated with [^{13}C,^{15}N]cyanide have an increased ratio of [^{13}C,^{15}N]Hcit/Hcit (0.011 ± 0.003) in the atheroma plaques compared with animals treated with PBS (ratio of 0.0009 ± 0.0005, $p < 0.01$). Labeled cyanide was used because carbamylation naturally occurs *in vivo*. Labeling with [^{13}C,^{15}N]Hcit allowed us to demonstrate that chronic exposure to cyanide causes carbamylation via MPO activity. In this context, the ratio of [^{13}C,^{15}N]Hcit/Hcit was the preferred readout to express carbamylation. On the other hand, [^{13}C,^{15}N]Hcit was too low in plasma, cell pellets, and supernatant of peritoneal lavages and was not detected. Nevertheless, it is worth noting that Hcit levels in atheroma plaques were the same in the cyanide hMPO-TG-LDLR$^{-/-}$ mice and PBS control hMPO-TG-LDLR$^{-/-}$ mice (Fig. 6*B*), showing that it is the chronic exposure to cyanide that led to increased carbamylation by MPO-dependent processes.

Figure 4. Mass spectrometric analyses. *A*, oxidation of cyanide by the MPO/H_2O_2 system. The isotopomers of $^-$CN (final concentration = 1 mM) were mixed with H_2O_2 (1 mM) in 10 mM ammonium acetate buffer, pH 7.4, and the reaction was started with 0.3 μM human recombinant MPO at 37 °C with a reaction time of 1 h. $^-$OCN, $^-$O^{13}CN, and $^-$O^{13}C^{15}N peaks (at 41.9997, 43.0030, and 43.9999 *m*/*z*, respectively) could be detected, which correspond to the oxidation products of cyanide isotopes. Spectra have been generated by subtracting spectra of a blank (buffer alone). *B*, taurine carbamylation. Taurine (1 mM) was mixed with 0.3 μM human recombinant MPO and isotopic cyanide (1 mM) for 12 h (37 °C) in 10 mM ammonium acetate buffer, pH 7.4, and the reaction was started with 1 mM H_2O_2. A peak was detected at *m*/*z* of 167.0109, which corresponds to [^{12}C]carbamyltaurine and MS/MS spectra fit with those of the control. In similar experiments with isotopomers, peaks were detected at *m*/*z* = 168.0284 and 169.0155, which correspond to ^{13}C- and ^{13}C,^{15}N-labeled carbamyltaurine. *C*, MS and MS/MS spectra of carbamyltaurine obtained after mixing taurine (1 mM) and cyanate (1 mM) in the acetate buffer and overnight incubation. *D*, MS and MS/MS spectra for the reaction of taurine chloramines (formed by mixing of 0.5 mM HOCl and 1 mM taurine) with ^{12}C- and ^{13}C-labeled thiocyanate after a reaction time of 12 h. Peaks detected at *m*/*z* values 167.0115 and 168.0160 correspond to ^{12}C- and ^{13}C-labeled carbamyltaurine (absent in the taurine chloramine MS spectra). Their identity was confirmed by MS/MS experiments (*D*, *inset*).

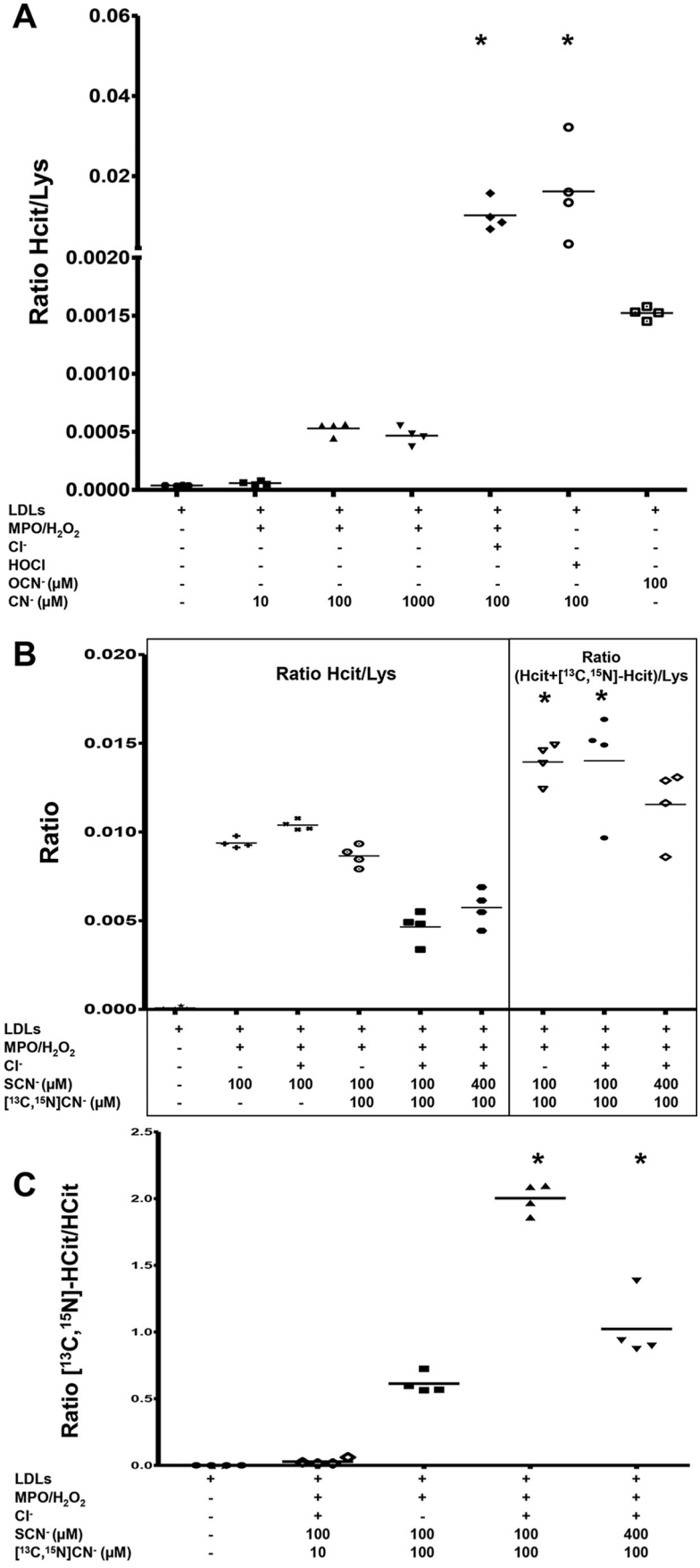
A
Ratio Hcit/Lys
0.06
0.04
0.02
0.0020
0.0015
0.0010
0.0005
0.0000
LDLs + + + + + + +
MPO/H2O2 - + + + + - -
Cl- - - - - + - -
HOCl - - - - - + -
OCN- (μM) - - - - - - 100
CN- (μM) - 10 100 1000 100 100 -
B
Ratio
Ratio Hcit/Lys
Ratio (Hcit+[13C,15N]-Hcit)/Lys
0.020
0.015
0.010
0.005
0.000
LDLs + + + + + + + + +
MPO/H2O2 - + + + + + + + +
Cl- - - + - + + - + +
SCN- (μM) - 100 100 100 100 400 100 100 400
[13C,15N]CN- (μM) - - - 100 100 100 100 100 100
C
Ratio [13C,15N]-HCit/HCit
2.5
2.0
1.5
1.0
0.5
0.0
LDLs + + + + +
MPO/H2O2 - + + + +
Cl- - + - + +
SCN- (μM) - 100 100 100 400
[13C,15N]CN- (μM) - 10 100 100 100

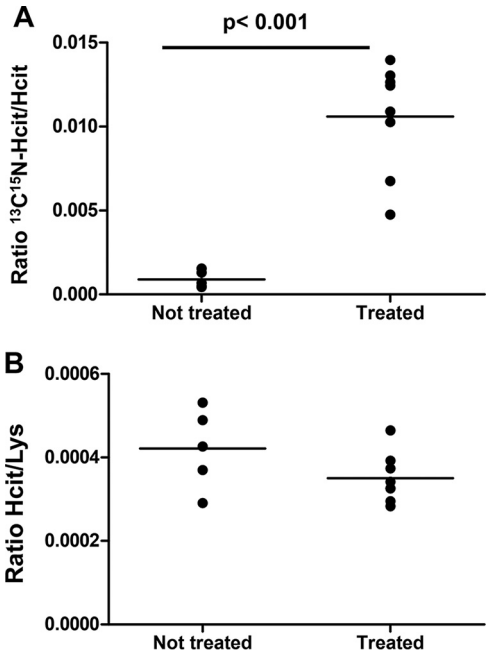

Figure 6. *In vivo* effect of cyanide. Exposure of hMPO-TG-LDLR$^{-/-}$ mice to [^{13}C,^{15}N]cyanide (0.4 mg/kg/day) led to protein-bound [^{13}C,^{15}N]Hcit formation in atheroma plaque. Mice were exposed for 8 weeks to isotope-labeled cyanide ($n = 8$) or to PBS (control, $n = 5$). Protein-bound Lys, Hcit, and [^{13}C,^{15}N]Hcit were monitored, and [^{13}C,^{15}N]Hcit/Hcit (*A*) and Hcit/Lys (*B*) ratios were calculated. A statistically significant difference was observed between groups (*t* test, $p < 0.001$).

Discussion

Mounting evidence for the involvement of MPO in atherogenesis has emerged for the past decades. It is now accepted that MPO catalyzes oxidation reactions via the release of reactive halogenating and nitrating species that render LDL atherogenic and high-density lipoprotein dysfunctional (28–33). In mice, Wang *et al.* (7) showed a marked increase in the content of protein-bound homocitrulline at atherosclerotic plaque-laden aortas of human MPO-transgenic mice as compared with nontransgenic counterparts. In both clinical and experimental *in vivo* situations, MPO seems to be a major catalytic component.

The enhanced consumption of hydrogen peroxide in the presence of low cyanide concentrations and the strict concentration dependence of compound I reduction unequivocally demonstrate the role of cyanide as electron donor for MPO. The inability of cyanide to promote the transition of compound I into compound II fits with the high one-electron reduction potential of the $^{\bullet}CN/^{-}CN$ couple (1.9 V) (20) that is significantly higher than that of the redox couple compound I/compound II (1.35 V) (34).

The observed spectral transition (Fig. 1*C*) can be explained by the following reaction sequence that involves cyanide as two-electron donor of compound I and as LS ligand for ferric MPO.

$$^{\cdot+}\text{PorFe(IV)=O} + {}^{-}\text{C}{\equiv}\text{N} \xrightarrow{k_2} \text{PorFe(III)} + {}^{-}\text{O–C}{\equiv}\text{N}$$

$$\text{PorFe(III)} + {}^{-}\text{C}{\equiv}\text{N} \xrightarrow{k_3} \text{PorFe(III)–C}{\equiv}\text{N}$$

Reactions 3 and 4

The calculated biomolecular rate of the reaction between cyanide and MPO(III) was determined to be $1.9 \times 10^6\ \text{M}^{-1}\ \text{s}^{-1}$ at pH 7.0 and 25 °C (k_3, Reaction 4). Because $k_3 > k_2$, the measured rate constant of the transition compound I → MPO(III) → LS MPO-cyanide complex reflects k_2 (Fig. 2). The two-electron oxidation of cyanide (k_2) is fast ($5.3 \times 10^5\ \text{M}^{-1}\ \text{s}^{-1}$ at pH 7.0 and 25 °C) and reflects the high oxidation capacity of MPO, which is the consequence of heme distortion due to unique heme-to-protein linkages, including an electron-withdrawing vinyl-sulfonium group (19). It is noteworthy that higher concentrations of cyanide favor the MPO-CN^- complex formation (k_3), limiting the MPO activation by reaction with H_2O_2 (k_1). Catalysis of the two-electron oxidation of cyanide by MPO is unique because related human peroxidases like LPO and EPO did not consume hydrogen peroxide in the presence of cyanide.

Mass spectrometric analyses have confirmed the production of cyanate derived from the two-electron oxidation of cyanide by compound I (see Fig. 2). This was supported by consecutive carbamylation reactions of produced cyanate with ϵ-amino groups of taurine and of free or LDL-bound lysine (Figs. 3–5). However, quantitative MS analyses also demonstrated that only 13% of cyanide was converted to cyanate by the MPO/H_2O_2/cyanide system (Fig. 4*A*). Nevertheless, the incubation of cyanide with HOCl (same concentration as hydrogen peroxide; 1 mM) converted only 20% of the cyanide to cyanate. It is also noteworthy that higher concentrations of cyanide (*e.g.* 1 mM) did not increase LDL carbamylation, which corroborates the kinetic studies (Fig. 5*A*).

In addition, the present work suggests further new routes of carbamylation, namely cyanate formation by HOCl-mediated cyanide oxidation and/or by reaction of stable chloramines with thiocyanate (35, 36). Both pathways follow reactions that only indirectly depend on MPO. Chloramines are relatively stable derivatives and are produced by the reaction of amines with HOCl released from MPO at sites of inflammation (37). In addition to thiocyanate oxidation (7), our findings show that MPO can promote carbamylation in three additional ways: (i) by direct oxidation of cyanide, (ii) by reaction of hypochlorous

Figure 5. Formation of carbamylated LDL. *A*, box-whisker plots (5th to 95th percentile) showing the ratios between Hcit and Lys residues (ratio Hcit/Lys), including conditions using only cyanide as substrate. *B*, box-whisker plots (5th to 95th percentile) showing the ratios between Hcit and Lys residues (ratio Hcit/Lys), including conditions using thiocyanate (SCN^-) and labeled cyanide ([^{13}C,^{15}N]CN^-). *Left*, only monoisotopic Hcit (unlabeled) is considered; *right*, total Hcit is considered (Hcit + [^{13}C,^{15}N]Hcit). *C*, box-whisker plots showing the ratios between labeled homocitrulline ([^{13}C,^{15}N]Hcit) and Hcit (ratio [^{13}C,^{15}N]Hcit/Hcit). Native LDLs were incubated overnight at 37 °C in buffer (10 mM phosphate, pH 7.4) in the presence of MPO (300 nM), H_2O_2 (1 mM), and/or chloride anions (150 mM) and/or HOCl (1 mM) and/or thiocyanate (SCN^-, 100 or 400 μM) and/or cyanide (CN^-) and/or [^{13}C,^{15}N]cyanide ([^{13}C,^{15}N]CN^-). LDLs were then delipidated, hydrolyzed by microwave under acidic conditions. Amino acid residues were labeled and, finally, analyzed using LC-MS/MS. Each condition was performed in quadruplicate ($n = 4$). *, statistically significant difference with the native LDL condition (Kruskal–Wallis, $p < 0.01$).

acid with cyanide, or (iii) by reaction of chloramines with thiocyanate.

In vivo, several anions compete with cyanide for reaction with MPO compound I, including chloride (150 mM) and thiocyanate (10–500 μM). We observed that in the presence of chloride, thiocyanate, and cyanide, carbamylation of lysine residues was mediated by oxidation of both thiocyanate and cyanide (Fig. 5*B*). In the presence of 100 μM concentrations of both thiocyanate and cyanide, about one-third of carbamylation derived from thiocyanate and two-thirds from cyanide oxidation (Fig. 5, *B* and *C*). Furthermore, higher concentration of thiocyanate (400 μM) decreased the carbamylation mediated by cyanide, but this was compensated by carbamylation mediated by thiocyanate. Under these conditions, the production of HOCl by MPO is lower than the production of HOSCN. However, the quantitative determination of Hcit demonstrated that only ~0.4% of thiocyanate and cyanide were involved in Hcit formation. Nevertheless, the carbamylation observed in LDLs is about 6 times higher compared with the addition of cyanate only (Fig. 5, *A* and *B*). Altogether, these data show a synergic effect of thiocyanate, cyanide, and chloride in the carbamylation process. This synergy might reflect previous reports about the reaction of cyanide with hypothiocyanate to a dicyanosulfide intermediate (36).

It remains to be discussed whether these reactions are relevant *in vivo*. MPO and $^{-}$CN do exist in soluble forms in blood, and the concentration ratios between these molecules used in the above experiments match those reported in human blood (*e.g.* [$^{-}$CN]/[MPO] ratio ~400:800, although the relative concentrations may vary depending on physiopathological conditions (*e.g.* chronic or acute inflammation, diet, and smoking) (38). Indeed, each cigarette can lead to exposure to 18–1500 μg of cyanide (10). However, the concentration measured in plasma even of smokers remains between 0.1 and 1.8 μM (39). But this can be explained by the rapid complexation and thiocyanate transformation (see also below). This led us to investigate the impact of chronic exposure to cyanide in a mouse model that expresses human MPO. The results of these experiments demonstrate that the postulated pathways are relevant *in vivo*. Protein-bound [^{13}C,^{15}N]homocitrulline was indeed increased in hMPO-TG-LDLR$^{-/-}$ mice that were exposed to labeled cyanide. Of importance, this increase was observed in atheroma plaque, where MPO and chronic inflammation are present (27), but not in plasma or in the peritoneal lavages (cell pellets and protein supernatant) during the acute inflammation process. These results show that cyanide is involved in chronic inflammatory processes by promoting the accumulation of protein-bound Hcit in atheroma plaque but is definitely not the preferred pathway in acute processes. Moreover, the absence of protein-bound [^{13}C,^{15}N]homocitrulline in plasma could reflect a dilution effect, making this marker undetectable. Moreover, cyanide oxidation by MPO in plasma may be affected by natural MPO inhibitors, such as the plasma metalloenzyme ceruloplasmin, anti-MPO Igs, and components of the complement system (40). Finally, it is important to highlight that the experiments have been carried out based on a theoretical cyanide exposure of 5 μg/day for 8 weeks, which could lead to submicromolar concentration of cyanide in blood. A better monitoring of cyanide exposure correlated to blood concentrations should help in understanding the impact of cyanide exposure on cardiovascular diseases.

On the other hand, cyanide is known to be rapidly metabolized by three main routes (41): (i) production of 2-amino-4-thiazoline carboxylic acid from cysteine and $^{-}$CN, (ii) synthesis of cyanocobalamin (CN-B12) via binding to vitamin B12 analogues (*e.g.* hydroxycobalamin or methylcobalamin), and (iii) transformation into thiocyanate by a thiosulfate sulfurtransferase in the presence of a sulfur donor, such as thiosulfate (42). All of these reactions hamper the quantification of MPO-mediated cyanide oxidation *in vivo* as well as of HOCl-mediated cyanide oxidation. However, they have no impact on carbamylation mediated by chloroamines and thiocyanate. The plasma concentration of the latter is known to be modulated by diet and smoking (7).

Summing up, this is the first work describing cyanide as a substrate for a peroxidase, thereby changing the perception of heme protein–cyanide interaction. The presented data also suggest new pathways of cyanate formation and protein carbamylation *in vivo* that involve MPO either directly or its reaction products hypochlorous acid and/or chloramines. The *in vivo* experiments show that chronic exposure to cyanide promotes the accumulation of carbamylated protein by multiple chemical pathways in atheroma plaque in a mouse model that mimics cardiovascular risk. Chronic exposure to air pollutants produced by combustion of organic materials (*e.g.* industrial and motor combustions) is reported to increase physiological levels of cyanide (10, 43–45), and recent data confirm the link between air pollution and cardiovascular risk (46–48). Future studies should explore the impact of MPO on oxidation of cyanide derived from pollution or tobacco smoke in human cardiovascular diseases.

Experimental procedures

Materials and reagents

Experiments were performed using both leukocyte and recombinant MPO for which no differences in kinetics of transitions were observed within experimental errors (49). Highly purified MPO of a purity index (A_{430}/A_{280}) of at least 0.85 was purchased from Planta Natural Products. Transfection of recombinant plasmids into Chinese hamster ovary cells, selection, culture procedures, and protein purification protocols were described previously (50). The recombinant protein had a purity index (A_{430}/A_{280}) of about 0.7. Generally, concentration of MPO was calculated using $\epsilon_{430\,nm} = 91\ mM^{-1}\ cm^{-1}$ as described previously (51). Eosinophil peroxidase was purified as described (52). Bovine lactoperoxidase and HRP were from Sigma-Aldrich Handels GmbH (Vienna, Austria). Hydrogen peroxide (H_2O_2) concentration was determined spectrophotometrically at 240 nm ($\epsilon = 39.4\ M^{-1}\ cm^{-1}$) (53).

LDLs were isolated from human plasma by ultracentrifugation according to Havel *et al.* (54). This study conforms with the Declaration of Helsinki, and its protocol was approved by the Ethics Committee of "CHU de Charleroi." Finally, all subjects gave their written informed consent. Before modification, the LDL fraction ($1.019 < d < 1.067$ g/ml) was desalted by two

consecutive passages through PD10 gel-filtration columns (Amersham Biosciences) using phosphate buffer (10 mM, pH 7.4). The different steps were carried out in the dark, and the protein concentration was measured by an ELISA kit for apoB-100 measurement.

Amperometric analysis of hydrogen peroxide consumption

Hydrogen peroxide consumption by MPO was measured by amperometry using a combined platinum/reference electrode (covered with a hydrophilic membrane) fitted to an Amperometric Biosensor Detector 3001 (Universal Sensors, Inc.). The applied electrode potential at pH 7.4 was 650 mV, and the H_2O_2 electrode-filling solution was freshly prepared twice daily. The electrode was calibrated against known concentrations of H_2O_2. Consumption of H_2O_2 (100 μM) in 100 mM phosphate buffer, pH 7.4, was followed (25 °C), and reactions were started by the addition of either 500 nM MPO, EPO, or LPO.

Transient-state experiments

Multimixing stopped-flow measurements were performed with an SX-18MV spectrofluorometer (Applied Photophysics). As soon as 100 μl were shot into a flow cell having a 1-cm light path, the fastest time for mixing the solution and recording the first data point was 1.3 ms. The reactions were followed both at fixed wavelength and by using a diode-array detector. At least three determinations (2000 data points) of pseudo-first-order rate constants (k_{obs}) were performed for each substrate concentration (pH 7.0, 25 °C). The mean value was used in the calculation of the second-order rate constants obtained from the slope of the plot of k_{obs} *versus* substrate concentration. Concentrations of substrates were at least 10 times in excess as compared with that of the enzyme.

Due to the inherent instability of compound I of MPO, the sequential stopped-flow (multimixing) technique was used for determination of rates of reaction of compound I with cyanide. Typically, MPO (8 μM) was premixed with a 10-fold excess of H_2O_2 in the aging loop for 30 ms (100 mM phosphate buffer, pH 7.0). LPO and HRP (8 μM) were premixed with an equimolar concentration of hydrogen peroxide for 100 and 1200 ms, respectively. Finally, compound I was allowed to react with varying concentrations of cyanide. Cyanide oxidation was followed by monitoring the absorbance change at 456 nm (MPO), 430 nm (LPO), and at 403 nm (HRP), respectively.

All reactions were also investigated using the diode-array detector (Applied Photophysics PD.1) attached to the stopped-flow machine. Normal data sets were analyzed using the Pro-K simulation program from Applied Photophysics, which allowed the synthesis of artificial sets of time-dependent spectra as well as spectral analysis of enzyme intermediates.

Carbamylation assays, product analysis, and Hcit quantitation by MS

Cyanate production was carried out at 37 °C in a final volume of 1.0 ml. The reaction mixture contained the following reagents at the final concentrations indicated in parentheses: ammonium acetate buffer, pH 7.4 (10 mM), H_2O_2 (1 mM), and cyanide (1 mM). The reaction was started by the addition of MPO (300 nM). Alternatively, cyanate was obtained by mixing isotopomers of cyanide (1 mM) and HOCl (1 mM) in the same buffer. Cyanate concentration was calculated to a calibration curve from 50 to 1000 μM KOCN. After incubation for 1 h, the solution was analyzed by MS using an infusion system within an Agilent (Palo Alto, CA) 6520 ESI source QTOF mass spectrometer in negative mode with a source temperature at 325 °C, a VCap at 4500 V, a drying gas at 5 liters/min, a nebulizer gas at 10 p.s.i.g., a fragmentor at 150 V, and a skimmer at 80 V. Spectra were accumulated for 2 min.

Tandem MS/MS analysis of the cyanate production was carried out by infusion on a Quattro premier XE (Waters, Milford, MA) using an electrospray in negative mode with a source temperature at 120 °C, a desolvation temperature at 400 °C, a gas flow at 503 liters/h, a capillary voltage at 2.5 kV, and a cone voltage at 50 V. The fragmentation was allowed with collision energy at 90 eV. The spectra are the results of 30 accumulated scans.

Reactions of carbamylation were performed in triplicate in 10 mM ammonium acetate buffer, pH 7.4, at 37 °C with recombinant MPO. Usually a 50:50 methanol/solution mixture was directly infused (0.3 ml/min) into the Agilent QTOF described above, and spectra were accumulated for 2 min.

Carbamylation of taurine or lysine was performed using a mixture of taurine (1 mM) or lysine (1 mM), MPO (300 nM), and cyanide (1 mM) in ammonium acetate buffer, pH 7.4 (37 °C), and the reaction was started by the addition of H_2O_2 (1 mM).

Chlorotaurine was produced by mixing taurine (1 mM) with HOCl (500 μM) at 37 °C. After 4 h, cyanide (1 mM) or thiocyanate (1 mM) was added. After 12 h, carbamyltaurine and homocitrulline formation was analyzed in negative mode on the ESI-QTOF described above with a source temperature at 325 °C, a VCap at 4000 V, a drying gas at 5 liters/min, a nebulizer gas at 10 p.s.i.g., a fragmentor at 165 V, and a skimmer at 80 V. MS/MS spectra were obtained by monitoring the collision energy at 1 V. Analysis of carbamyllysine was performed with the same specifications but in positive mode. Standard solutions were obtained by mixing in taurine (1 mM) or lysine (1 mM) with cyanate (1 mM) at 37 °C under identical conditions (incubation time of 12 h).

LDLs (1 mg/ml) were isolated by standard protocol (54) and were incubated overnight in phosphate buffer (10 mM), pH 7.4 (37 °C), with MPO (300 nM) and cyanide (10, 100, or 1000 μM) with or without chloride (150 mM). The reaction was started by the addition of H_2O_2 (1 mM). A control condition without MPO but with H_2O_2 (1 mM) and cyanide (100 μM) was also performed. LDLs (1 mg/ml) were also incubated with phosphate buffer (10 mM), pH 7.4 (37 °C), and cyanide (100 μM) before the addition of HOCl (1 mM). A positive control where LDLs (1 mg/ml) were incubated overnight in the same buffer in the presence of cyanate (100 μM) at 37 °C was performed. LDLs (1 mg/ml) were also incubated for 4 h (37 °C) with HOCl (1 mM) in phosphate buffer (10 mM), pH 7.4 (37 °C), before the addition of thiocyanate (100 μM) and overnight incubation. Finally, LDLs (1 mg/ml) were incubated overnight (37 °C) in phosphate buffer (10 mM), pH 7.4 (37 °C), with MPO (300 nM), chloride anions (150 mM), thiocyanate (100 or 400 μM), and [^{13}C,^{15}N] cyanide (10 or 100 μM).

Native LDL and carbamyl-LDL were precipitated with TCA (10%) and centrifuged for 10 min at 16,000 × *g*. Supernatant was discarded, and the process was repeated one more time. The precipitate was then mixed with a solution of water/methanol/diethylic ether (1:3:7) to remove lipids. The mixture was centrifuged 10 min at 16,000 × *g*, the supernatant was discarded, and the process was repeated. The obtained pellets were dried down using a vacuum centrifuge before acid hydrolysis, derivatization, and MS/MS analysis. The latter was carried out as described below.

Carbamylation was monitored by LC-MS/MS after acidic hydrolysis as described previously (55). [^{13}C,^{15}N]Lysine (3.4 μM, final concentration) was added as an internal standard. Acid hydrolysis was carried out at 110 °C using a microwave oven; resulting amino acid residues were labeled, and samples were cleaned up as described previously (55). At the end of the process, samples were reconstituted in 0.1% formic acid and injected into a 1290 Infinity series UHPLC system (Agilent Technologies, Palo Alto, CA). Amino acid residues were resolved on a Poroshell 120 EC-C18 column (2.1 × 100 mm, 2.7 μm) (Agilent Technologies) using a gradient of 0.2% formic acid and methanol. Lys, Hcit, and [^{13}C,^{15}N]Hcit residues were quantified by tandem MS on a 6490 series ESI-triple quadrupole mass spectrometer using a JetStream source (Agilent Technologies, Palo Alto, CA). Parameters were as follows: positive mode; dynamic MRM; gas temperature of 250 °C; drying gas of 14 liters/min; nebulizer pressure of 20 p.s.i.g.; sheath gas heater at 350 °C; sheath gas flow of 7 liters/min; capillary voltage of 3000 V; high-pressure RF of 150 V; low pressure RF of 60 V; fragmentor at 380 V. Fixed collision energies (CEs) were optimized for each residue and for each product ion and were as follows: Hcit, precursor ion *m*/*z* of 246.2, quantifier product ion = 229.1 using CE = 9 V, qualifier product ion = 84.1 using CE = 25 V; [^{13}C,^{15}N]Hcit: precursor ion *m*/*z* of 248.2, quantifier product ion = 230.1 using CE = 9 V, qualifier product ion = 84.1 using CE = 25 V; Lys: precursor ion *m*/*z* of 203.2, quantifier product ion = 186.2 using CE = 9 V, qualifier product ion = 84.1 using CE = 13 V. The precursor ions correspond to the butanolic esters of the amino acid residues. Precursor isolation mode was in unit mode for Lys and enhanced mode for Hcit and [^{13}C,^{15}N]Hcit. For the quantitation of Hcit in samples, a standard curve of Hcit was performed from 1 to 10,000 nM, and [^{13}C,^{15}N]lysine was used as an internal standard. Data were acquired using MassHunter Acquisition® software and analyzed by MassHunter Quantitative Analysis® software (version B.07, Agilent Technologies).

Animals

Age- and sex-matched C57BL/6, human MPO transgenics (−463G allele) (hMPO-TG), and hMPO-TG crossed to the LDLR$^{-/-}$ mice on the C57BL/6 background were used in these studies. All animal experiments adhered to the *Guide for the Care and Use of Laboratory Animals* (56) and were performed using approved protocols from the Animal Research Committee at Sanford Burnham Prebys Medical Discovery Institute.

Potassium cyanide exposure of mice

Mice were fed a high-fat atherogenic diet (42% kcal from fat) (Envigo, TD 88137) for 12 weeks. After 4 weeks on a high-fat diet, the mice were randomly allocated to treated or control groups. Mice in the first group were injected intraperitoneally with potassium [^{13}C,^{15}N]cyanide (0.4 mg/kg, ~5 μg/day) in PBS every day for 8 weeks. Control mice were injected with PBS. Blood collection at sacrifice was by cardiac puncture under Avertin® anesthetic. Serum was prepared by centrifugation and stored at −80 °C until analyzed. The mice were then perfused with ice-cold PBS through the left ventricle, and proximal aortae were carefully dissected to remove adventitial fat. The region of the aorta containing the plaque was removed and frozen at −80 °C until analyzed. The brain, liver, and kidney were also collected and stored at −80 °C until analyzed.

Mouse model of inflammation

The procedure for inflammation was performed essentially as described by Wang *et al.* (7) except that in this study, we injected potassium [^{13}C,^{15}N]cyanide. Briefly, animals were injected intraperitoneally with 1 ml of 4% thioglycollate broth. Twenty hours later, mice were injected with zymosan (250 mg/kg) and potassium [^{13}C,^{15}N]cyanide (1.6 mg/kg). Peritoneal lavage was performed 4 h later with PBS containing 100 μM butylated hydroxytoluene and 100 μM diethylenetriaminepentaacetic acid. The samples were centrifuged at 1000 rpm for 5 min at 4 °C to separate the lavage fluid from the peritoneal cells. The samples were frozen and stored at −80 °C until analyzed.

Statistics

Data were analyzed using SigmaPlot® version 12.0 software. Mean values with S.D. were reported because the data were normally distributed (normality tests, Shapiro-Wilk passed). Parametric *t* tests were the most appropriate for our study design. Outcomes were considered as statistically significant with a two-tailed $p < 0.05$. Based on six preliminary mice (treated *versus* nontreated, difference on mean and S.D.), we determined the number of mice to obtain a power of performed two-tailed test (with $\alpha = 0{,}050$) to 0.8. No mice were excluded from the study.

The operator was blinded, as each sample was allocated to a code number, and the corresponding group was revealed after LC-MS data analyses and before statistical analysis.

Author contributions—P. V. A., C. D., P. G. F., R. A. M., W. F. R., V. N., M. D., B. R., A. R., C. N., D. D., F. R., C. C., and M. S. performed experiments; P. V. A., C. D., K. Z. B., W. F. R., R. A. M., P. G. F., L. V., and C. O. designed experiments and analyzed data; C. D., P. V. A., K. Z. B., P. G. F., R. A. M., W. F. R., M. R., N. M., M. V., J. D., J. N. and C. O. wrote the manuscript; K. Z. B., B. R., W. F. R., R. A. M., and P. V. A. provided reagents, notably recombinant MPO, materials, and analysis tools.

Acknowledgment—We thank Dr. Kjell Mortier (Waters, Zeelik, Belgium) for helpful advice on the Quattro Premier XE instrument.

References

1. Zeng, J. (1991) Lysine modification of metallothionein by carbamylation and guanidination. *Methods Enzymol.* **205,** 433–437 CrossRef Medline

2. Golemi, D., Maveyraud, L., Vakulenko, S., Samama, J. P., and Mobashery, S. (2001) Critical involvement of a carbamylated lysine in catalytic function of class D β-lactamases. *Proc. Natl. Acad. Sci. U.S.A.* **98,** 14280–14285 CrossRef Medline
3. Kraus, L. M., Jones, M. R., and Kraus, A. P., Jr. (1998) Essential carbamoyl-amino acids formed *in vivo* in patients with end-stage renal disease managed by continuous ambulatory peritoneal dialysis: isolation, identification, and quantitation. *J. Lab. Clin. Med.* **131,** 425–431 CrossRef Medline
4. Kraus, L. M., and Kraus, A. P., Jr. (2001) Carbamoylation of amino acids and proteins in uremia. *Kidney Int. Suppl.* **78,** S102–S107 CrossRef Medline
5. Ok, E., Basnakian, A. G., Apostolov, E. O., Barri, Y. M., and Shah, S. V. (2005) Carbamylated low-density lipoprotein induces death of endothelial cells: a link to atherosclerosis in patients with kidney disease. *Kidney Int.* **68,** 173–178 CrossRef Medline
6. Jaisson, S., Lorimier, S., Ricard-Blum, S., Sockalingum, G. D., Delevallée-Forte, C., Kegelaer, G., Manfait, M., Garnotel, R., and Gillery, P. (2006) Impact of carbamylation on type I collagen conformational structure and its ability to activate human polymorphonuclear neutrophils. *Chem. Biol.* **13,** 149–159 CrossRef Medline
7. Wang, Z., Nicholls, S. J., Rodriguez, E. R., Kummu, O., Hörkkö, S., Barnard, J., Reynolds, W. F., Topol, E. J., DiDonato, J. A., and Hazen, S. L. (2007) Protein carbamylation links inflammation, smoking, uremia and atherogenesis. *Nat. Med.* **13,** 1176–1184 CrossRef Medline
8. Zamocky, M., Jakopitsch, C., Furtmüller, P. G., Dunand, C., and Obinger, C. (2008) The peroxidase-cyclooxygenase superfamily: reconstructed evolution of critical enzymes of the innate immune system. *Proteins* **72,** 589–605 CrossRef Medline
9. Nicholls, S. J., and Hazen, S. L. (2005) Myeloperoxidase and cardiovascular disease. *Arterioscler. Thromb. Vasc. Biol.* **25,** 1102–1111 CrossRef Medline
10. Mahernia, S., Amanlou, A., Kiaee, G., and Amanlou, M. (2015) Determination of hydrogen cyanide concentration in mainstream smoke of tobacco products by polarography. *J. Environ. Health Sci. Eng.* **13,** 57 CrossRef Medline
11. Abraham, K., Buhrke, T., and Lampen, A. (2016) Bioavailability of cyanide after consumption of a single meal of foods containing high levels of cyanogenic glycosides: a crossover study in humans. *Arch. Toxicol.* **90,** 559–574 CrossRef Medline
12. Cooper, C. E., and Brown, G. C. (2008) The inhibition of mitochondrial cytochrome oxidase by the gases carbon monoxide, nitric oxide, hydrogen cyanide and hydrogen sulfide: chemical mechanism and physiological significance. *J. Bioenerg. Biomembr.* **40,** 533–539 CrossRef Medline
13. Marquez, L. A., and Dunford, H. B. (1989) Cyanide binding to canine myeloperoxidase. *Biochem. Cell Biol.* **67,** 187–191 CrossRef Medline
14. Bolscher, B. G., and Wever, R. (1984) A kinetic study of the reaction between human myeloperoxidase, hydroperoxides and cyanide: inhibition by chloride and thiocyanate. *Biochim. Biophys. Acta* **788,** 1–10 CrossRef Medline
15. Ikeda-Saito, M. (1987) A study of ligand binding to spleen myeloperoxidase. *Biochemistry* **26,** 4344–4349 CrossRef Medline
16. Dolman, D., Dunford, H. B., Chowdhury, D. M., and Morrison, M. (1968) The kinetics of cyanide binding by lactoperoxidase. *Biochemistry* **7,** 3991–3996 CrossRef Medline
17. Palcic, M. M., and Dunford, H. B. (1981) The kinetics of cyanide binding by human erythrocyte catalase. *Arch. Biochem. Biophys.* **211,** 245–252 CrossRef Medline
18. Chance, B. (1949) The reaction of catalase and cyanide. *J. Biol. Chem.* **179,** 1299–1309 Medline
19. Furtmüller, P. G., Zederbauer, M., Jantschko, W., Helm, J., Bogner, M., Jakopitsch, C., and Obinger, C. (2006) Active site structure and catalytic mechanisms of human peroxidases. *Arch. Biochem. Biophys.* **445,** 199–213 CrossRef Medline
20. Arnhold, J., Monzani, E., Furtmüller, P. G., Zederbauer, M., Casella, L., and Obinger, C. (2006) Kinetics and thermodynamics of halide and nitrite oxidation by mammalian heme peroxidases. *Eur. J. Inorg. Chem.* **2006,** 3801–3811 CrossRef
21. Jantschko, W., Georg Furtmüller, P., Zederbauer, M., Lanz, M., Jakopitsch, C., and Obinger, C. (2003) Direct conversion of ferrous myeloperoxidase to compound II by hydrogen peroxide: an anaerobic stopped-flow study. *Biochem. Biophys. Res. Commun.* **312,** 292–298 CrossRef Medline
22. Furtmüller, P. G., Burner, U., Regelsberger, G., and Obinger, C. (2000) Spectral and kinetic studies on the formation of eosinophil peroxidase compound I and its reaction with halides and thiocyanate. *Biochemistry* **39,** 15578–15584 CrossRef Medline
23. Furtmüller, P. G., Jantschko, W., Regelsberger, G., Jakopitsch, C., Arnhold, J., and Obinger, C. (2002) Reaction of lactoperoxidase compound I with halides and thiocyanate. *Biochemistry* **41,** 11895–11900 CrossRef Medline
24. Grisham, M. B., Jefferson, M. M., Melton, D. F., and Thomas, E. L. (1984) Chlorination of endogenous amines by isolated neutrophils. Ammonia-dependent bactericidal, cytotoxic, and cytolytic activities of the chloramines. *J. Biol. Chem.* **259,** 10404–10413 Medline
25. Malle, E., Marsche, G., Arnhold, J., and Davies, M. J. (2006) Modification of low-density lipoprotein by myeloperoxidase-derived oxidants and reagent hypochlorous acid. *Biochim. Biophys. Acta* **1761,** 392–415 CrossRef Medline
26. Piedrafita, F. J., Molander, R. B., Vansant, G., Orlova, E. A., Pfahl, M., and Reynolds, W. F. (1996) An Alu element in the myeloperoxidase promoter contains a composite SP1-thyroid hormone-retinoic acid response element. *J. Biol. Chem.* **271,** 14412–14420 CrossRef Medline
27. Castellani, L. W., Chang, J. J., Wang, X., Lusis, A. J., and Reynolds, W. F. (2006) Transgenic mice express human MPO −463G/A alleles at atherosclerotic lesions, developing hyperlipidemia and obesity in −463G males. *J. Lipid Res.* **47,** 1366–1377 CrossRef Medline
28. Abu-Soud, H. M., and Hazen, S. L. (2000) Nitric oxide is a physiological substrate for mammalian peroxidases. *J. Biol. Chem.* **275,** 37524–37532 CrossRef Medline
29. Eiserich, J. P., Baldus, S., Brennan, M. L., Ma, W., Zhang, C., Tousson, A., Castro, L., Lusis, A. J., Nauseef, W. M., White, C. R., and Freeman, B. A. (2002) Myeloperoxidase, a leukocyte-derived vascular NO oxidase. *Science* **296,** 2391–2394 CrossRef Medline
30. Baldus, S., Heitzer, T., Eiserich, J. P., Lau, D., Mollnau, H., Ortak, M., Petri, S., Goldmann, B., Duchstein, H. J., Berger, J., Helmchen, U., Freeman, B. A., Meinertz, T., and Münzel, T. (2004) Myeloperoxidase enhances nitric oxide catabolism during myocardial ischemia and reperfusion. *Free Radic. Biol. Med.* **37,** 902–911 CrossRef Medline
31. Vita, J. A., Brennan, M. L., Gokce, N., Mann, S. A., Goormastic, M., Shishehbor, M. H., Penn, M. S., Keaney, J. F., Jr., and Hazen, S. L. (2004) Serum myeloperoxidase levels independently predict endothelial dysfunction in humans. *Circulation* **110,** 1134–1139 CrossRef Medline
32. Zheng, L., Nukuna, B., Brennan, M. L., Sun, M., Goormastic, M., Settle, M., Schmitt, D., Fu, X., Thomson, L., Fox, P. L., Ischiropoulos, H., Smith, J. D., Kinter, M., and Hazen, S. L. (2004) Apolipoprotein A-I is a selective target for myeloperoxidase-catalyzed oxidation and functional impairment in subjects with cardiovascular disease. *J. Clin. Invest.* **114,** 529–541 CrossRef Medline
33. Holzer, M., Gauster, M., Pfeifer, T., Wadsack, C., Fauler, G., Stiegler, P., Koefeler, H., Beubler, E., Schuligoi, R., Heinemann, A., and Marsche, G. (2011) Protein carbamylation renders high-density lipoprotein dysfunctional. *Antioxid. Redox Signal.* **14,** 2337–2346 CrossRef Medline
34. Berdnikov, V. M., and Bazhin, N. M. (1970) Oxidation-reduction potentials of certain inorganic radicals in aqueous solutions. *Russ. J. Phys. Chem.* **44,** 395–398
35. Xulu, B. A., and Ashby, M. T. (2010) Small molecular, macromolecular, and cellular chloramines react with thiocyanate to give the human defense factor hypothiocyanite. *Biochemistry* **49,** 2068–2074 CrossRef Medline
36. Lemma, K., and Ashby, M. T. (2009) Reactive sulfur species: kinetics and mechanism of the reaction of hypothiocyanous acid with cyanide to give dicyanosulfide in aqueous solution. *Chem. Res. Toxicol.* **22,** 1622–1628 CrossRef Medline
37. Pattison, D. I., Hawkins, C. L., and Davies, M. J. (2009) What are the plasma targets of the oxidant hypochlorous acid? A kinetic modeling approach. *Chem. Res. Toxicol.* **22,** 807–817 CrossRef Medline

38. Lundquist, P., Rosling, H., Sörbo, B., and Tibbling, L. (1987) Cyanide concentrations in blood after cigarette smoking, as determined by a sensitive fluorimetric method. *Clin. Chem.* **33,** 1228–1230 Medline
39. Cailleux, A., Subra, J. F., Riberi, P., Tuchais, E., Premel-Cabic, A., and Allain, P. (1988) Cyanide and thiocyanate blood levels in patients with renal failure or respiratory disease. *J. Med.* **19,** 345–351 Medline
40. Savenkova, M. L., Mueller, D. M., and Heinecke, J. W. (1994) Tyrosyl radical generated by myeloperoxidase is a physiological catalyst for the initiation of lipid peroxidation in low density lipoprotein. *J. Biol. Chem.* **269,** 20394–20400 Medline
41. Boxer, G. E., and Rickards, J. C. (1952) Studies on the metabolism of the carbon of cyanide and thiocyanate. *Arch. Biochem. Biophys.* **39,** 7–26 CrossRef Medline
42. Ansell, M., and Lewis, F. A. (1970) A review of cyanide concentrations found in human organs: a survey of literature concerning cyanide metabolism, "normal", non-fatal, and fatal body cyanide levels. *J. Forensic Med.* **17,** 148–155 Medline
43. Matti Maricq, M. (2007) Chemical characterization of particulate emissions from diesel engines: a review. *J. Aerosol Sci.* **38,** 1079–1118 CrossRef
44. Baum, M. M., Moss, J. A., Pastel, S. H., and Poskrebyshev, G. A. (2007) Hydrogen cyanide exhaust emissions from in-use motor vehicles. *Environ. Sci. Technol.* **41,** 857–862 CrossRef Medline
45. Moussa, S., Leithead, A., Li, S.-M., Chan, T., Wentzella, J., Stroud, C., Zhang, J., Lee, P., Lu, G., Brook, J., Hayden, K., Narayan, J., and Liggio, J. (2016) Emissions of hydrogen cyanide from on-road gasoline and diesel vehicles. *Atmos. Environ.* **131,** 185–195 CrossRef
46. Miller, M. R., Shaw, C. A., and Langrish, J. P. (2012) From particles to patients: oxidative stress and the cardiovascular effects of air pollution. *Future Cardiol.* **8,** 577–602 CrossRef Medline
47. Franchini, M., Guida, A., Tufano, A., and Coppola, A. (2012) Air pollution, vascular disease and thrombosis: linking clinical data and pathogenic mechanisms. *J. Thromb. Haemost.* **10,** 2438–2451 CrossRef Medline
48. Lucking, A. J., Lundbäck, M., Barath, S. L., Mills, N. L., Sidhu, M. K., Langrish, J. P., Boon, N. A., Pourazar, J., Badimon, J. J., Gerlofs-Nijland, M. E., Cassee, F. R., Boman, C., Donaldson, K., Sandstrom, T., Newby, D. E., and Blomberg, A. (2011) Particle traps prevent adverse vascular and prothrombotic effects of diesel engine exhaust inhalation in men. *Circulation* **123,** 1721–1728 CrossRef Medline
49. Furtmüller, P. G., Jantschko, W., Regelsberger, G., Jakopitsch, C., Moguilevsky, N., and Obinger, C. (2001) A transient kinetic study on the reactivity of recombinant unprocessed monomeric myeloperoxidase. *FEBS Lett.* **503,** 147–150 CrossRef Medline
50. Moguilevsky, N., Garcia-Quintana, L., Jacquet, A., Tournay, C., Fabry, L., Piérard, L., and Bollen, A. (1991) Structural and biological properties of human recombinant myeloperoxidase produced by Chinese hamster ovary cell lines. *Eur. J. Biochem.* **197,** 605–614 CrossRef Medline
51. Furtmüller, P. G., Burner, U., and Obinger, C. (1998) Reaction of myeloperoxidase compound I with chloride, bromide, iodide, and thiocyanate. *Biochemistry* **37,** 17923–17930 CrossRef Medline
52. Furtmüller, P. G., Jantschko, W., Regelsberger, G., and Obinger, C. (2001) Spectral and kinetic studies on eosinophil peroxidase compounds I and II and their reaction with ascorbate and tyrosine. *Biochim. Biophys. Acta* **1548,** 121–128 CrossRef Medline
53. Nelson, D. P., and Kiesow, L. A. (1972) Enthalpy of decomposition of hydrogen peroxide by catalase at 25 degrees C (with molar extinction coefficients of H_2O_2 solutions in the UV). *Anal. Biochem.* **49,** 474–478 CrossRef Medline
54. Havel, R. J., Eder, H. A., and Bragdon, J. H. (1955) The distribution and chemical composition of ultracentrifugally separated lipoproteins in human serum. *J. Clin. Invest.* **34,** 1345–1353 CrossRef Medline
55. Delporte, C., Franck, T., Noyon, C., Dufour, D., Rousseau, A., Madhoun, P., Desmet, J. M., Serteyn, D., Raes, M., Nortier, J., Vanhaeverbeek, M., Moguilevsky, N., Nève, J., Vanhamme, L., Van Antwerpen, P., and Zouaoui Boudjeltia, K. (2012) Simultaneous measurement of protein-bound 3-chlorotyrosine and homocitrulline by LC-MS/MS after hydrolysis assisted by microwave: application to the study of myeloperoxidase activity during hemodialysis. *Talanta* **99,** 603–609 CrossRef Medline
56. National Research Council of the National Academies (2011) *Guide for the Care and Use of Laboratory Animals*, 8th Ed., National Academies Press, Washington, D. C.